Received: 26 December 2021 | Revised: 16 March 2022 | Accepted: 12 April 2022

DOI: 10.1111/jcpe.13631

ORIGINAL ARTICLE

Journal of Clinical Periodontology WILEY

Excessive inflammatory response to infection in experimental peri-implantitis: Resolution by Resolvin D2

Oded Heyman[1] | Yael Horev[1] | Gabriel Mizraji[1] | Yaron Haviv[2] | Lior Shapira[1] | Asaf Wilensky[1]

[1]Department of Periodontology, Hadassah Medical Center, Faculty of Dental Medicine, Hebrew University of Jerusalem, Jerusalem, Israel

[2]Department of Oral Medicine, Sedation and Maxillofacial Imaging, Hadassah Medical Center, Faculty of Dental Medicine, Hebrew University of Jerusalem, Jerusalem, Israel

Correspondence
Asaf Wilensky, Department of Periodontology, Hadassah Medical Center, Faculty of Dental Medicine, Hebrew University of Jerusalem, P.O. Box 12272, Jerusalem 91120, Israel.
Email: asafw@ekmd.huji.ac.il

Funding information
Israel Science Foundation, Grant/Award Number: 2369/18

Abstract

Aim: The aetiology and pathogenesis of peri-implantitis are currently under active research. This study aimed to dissect the pathogenesis of murine experimental peri-implantitis and assess Resolvin D2 (RvD2) as a new treatment modality.

Materials and Methods: Four weeks following titanium implant insertion, mice were infected with *Porphyromonas gingivalis* using single or multiple oral lavages. RvD2 was administrated following infection, and tissues were analysed using flow cytometry, quantitative RT-PCR, taxonomic profiling, and micro-computed tomography.

Results: Repeated infections with *Pg* resulted in microbial dysbiosis and a higher influx of innate and adaptive leukocytes to the peri-implant mucosa (PIM) than to gingiva surrounding the teeth. This was accompanied by increased expression levels of IFN-α, IL-1β, and RANKL\OPG ratio. Interestingly, whereas repetitive infections resulted in bone loss around implants and teeth, a single infection induced bone loss only around implants, suggesting a higher susceptibility of the implants to infection. Treatment with RvD2 prevented *Pg*-driven bone loss and reduced leukocyte infiltration to the PIM.

Conclusions: Murine dental implants are associated with dysregulated local immunity and increase susceptibility to pathogen-induced peri-implantitis. However, the disease can be prevented by RvD2 treatment, highlighting the promising therapeutic potential of this treatment modality.

KEYWORDS
alveolar bone loss, dental implants, peri-implant mucosa, peri-implantitis, Resolvin D2

Clinical Relevance

Scientific rationale for study: The pathogenesis of peri-implantitis is still unclear. Using a murine model of experimental peri-implantitis, we examined the peri-implant mucosal immunity following infection and assessed the effect of resolving inflammation using Resolvin D2 (RvD2).

Principal findings: Dental implants present excessive inflammatory response following bacterial infection, compared to teeth, making them more susceptible to alveolar bone loss. Treatment

Jaccard/EFP research prize competition finalist.

with RvD2 prevented tissue damage by controlling the influx of neutrophils and by attenuating destructive immunity.

Practical implications: The data obtained regarding the pathogenesis of peri-implantitis and RvD2 will help us to proceed to human trials in the future.

1 | INTRODUCTION

Dental implants constitute an effective and widely used treatment modality for the prosthetic rehabilitation of missing teeth. However, the wide use of implants has brought in peri-implant diseases such as peri-implantitis. Peri-implantitis is an immune-mediated biological complication associated with the presence of peri-implant biofilm (Kotsakis & Olmedo, 2021). A recent systematic review and meta-analysis found that the weighted patient-based prevalence of peri-implantitis is 22% (Derks & Tomasi, 2015).

Similar to periodontitis, inflammation in the supporting tissues around implants results in tissue damage and bone loss (Berglundh et al., 2018). However, although the aetiology and pathogenesis of periodontitis have been studied extensively, the knowledge regarding peri-implantitis is still limited. Previous studies have shown that although both diseases share a similar phenotype, there are critical differences in clinical progression (Carcuac & Berglundh, 2014), histological characteristics (Carcuac & Berglundh, 2014), and microbial composition (Kumar et al., 2012), suggesting a different pathogenesis. This might explain the generally favourable response of periodontitis to anti-infective treatment, while the efficacy of this treatment to peri-implantitis is inadequate (Renvert et al., 2008). One major reason for the limited data regarding the pathogenesis of peri-implantitis is the difficulty of establishing a small-animal model. To tackle this problem, we and others recently reported the establishment of a murine model of dental implants and experimental peri-implantitis (Pirih et al., 2015; Koutouzis et al., 2017; Tzach-Nahman et al., 2017; Heyman et al., 2018). Using this model, we demonstrated that implants dysregulate immune response in the peri-implant mucosa (PIM). The inflammatory milieu contained higher levels of neutrophils, monocytes, lymphocytes, and RANKL-expressing $CD4^+$ T and B cells, together with high expression levels of pro-inflammatory cytokines and a high IL17A/Foxp3 ratio compared to control tissue surrounding the teeth (Heyman et al., 2018, 2020). This altered, inflamed condition in the PIM, referred to as "dysregulated homeostasis", may explain the increased susceptibility of implants in humans to infection and the consequent rapid deterioration of the supporting tissues (Carcuac & Berglundh, 2014; Salvi et al., 2017).

In recent years, specialized pro-resolving mediators (SPMs) have been suggested as therapeutic candidates for chronic inflammatory diseases, including periodontitis (Van Dyke, 2020). Resolvins, members of the SPMs family, are naturally occurring mediators of the resolution of inflammation that enhance host defence and actively promote tissue repair and bacterial clearance (Serhan et al., 2008). They also reduce the in vitro TNF-α and IFN-γ production by human $CD4^+$ and $CD8^+$ T cells (Chiurchiù et al., 2016), prevent the generation of activated Th1 and Th17 cells, and enhance the differentiation of regulatory T cells. Although resolvins have been used in small-animal models to control inflammation by lowering Th1 immunity, thereby preventing experimental periodontitis (Hasturk et al., 2007; Mizraji et al., 2018), the impact and efficacy of resolvins as therapy for peri-implantitis is still enigmatic.

To study the pathogenesis of peri-implantitis as compared to periodontitis, we used our previously described oral infection models to induce both diseases (Wilensky et al., 2015; Tzach-Nahman et al., 2017). Using these models, we found that implants are more susceptible to alveolar bone loss induced by oral infection. Suggested mechanisms involve a larger influx of leukocytes and corresponding overexpression of pro-inflammatory cytokines around diseased implants compared to infected teeth. The aim of this study was to expand our knowledge regarding the pathogenesis of peri-implantitis and propose an alternative treatment modality using Resolvin D2 (RvD2).

2 | MATERIALS AND METHODS

2.1 | Mice

A total of 188 female BALB/c mice (6–7 weeks old) were purchased from Envigo (Jerusalem, Israel). The animals were housed in a specific pathogen-free unit. All experimental procedures were reviewed and approved by the IACUC of the Hadassah-Hebrew University Medical Center.

2.2 | Tooth extraction and implant placement

The model design and surgery protocols used for this study have been previously described (Heyman et al., 2018) and are depicted in greater detail in Appendix S1. In brief, under full anaesthesia and analgesia, mice underwent extraction of the upper left molars. After 4 weeks of healing, two titanium implants (MIS Implants Technologies, Israel) were inserted.

2.3 | Experimental peri-implantitis and resolvin treatment protocol

Peri-implantitis was induced as previously described (Tzach-Nahman et al., 2017). Briefly, mice were infected via oral gavage once (40 mice) or three times (80 mice) at 2-day intervals, with 1×10^9 CFU of *Porphyromonas gingivalis* (*Pg*) 53,977 in 200 μl of 2% carboxymethyl cellulose solution (Sigma). One group of *Pg*-infected mice was treated with RvD2. Three doses of 0.5 μg RvD2 (Cayman Chemical) were administered i.p., every other day, followed by six i.p. doses of 0.1 μg every 2 days over the next 2 weeks (Figure 5a). For more details, see Appendix S1.

2.4 | Isolation and processing of the gingiva and peri-implant mucosal tissues and lymph nodes

The mucosal tissues and lymph nodes (LNs) were processed as previously reported (Heyman et al., 2018, 2020). In short, a circumference of 1 mm of gingiva around teeth or PIM surrounding implants, containing infiltrated connective tissue (ICT) and healthy tissue, were harvested. Tissues were minced, treated, stained, and analysed via flow cytometry, as depicted in detail in Appendix S1.

2.5 | RNA extraction and quantitative real-time polymerase chain reaction

RNA was isolated and served for cDNA synthesis using qScriptTM cDNA Synthesis Kit, (Quanta-BioSciences Inc.). RT-qPCR reaction was performed according to the manufacturer's instruction in a 20-μl reaction mixture using the Power SYBR Green PCR Master Mix (Quanta-BioSciences Inc.). For more details, see Appendix S1.

2.6 | Antibodies

The following fluorochrome-conjugated monoclonal antibodies were purchased from BioLegend: CD45.2 (104), I-A/I-E (M5/114.15.2), CD11b (M1/70), CD11c (N418), Ly6C (HK1.4), Ly6G (1A8), CD3 (17A2), CD4 (GK1.5), FOXP3 (MF-14), B220 (RA36B2) and RANKL (IK22/5), PDCA1/CD317 (927) and Siglec-H (551). Propidium iodide solution was also purchased from BioLegend.

2.7 | Micro-computed tomography analysis

The maxillae were scanned using a high-resolution scanner (μCT 40, Scanco Medical AG, Bassersdorf, Switzerland). A single examiner preformed three-dimensional analysis to evaluate bone loss around implants. The apical part of the implant's head served as a constant reference line for all samples in the sagittal plane. The centre of each implant was determined as the middle point of this reference line in the sagittal and axial planes. Next, a volume of interest in the shape of a box was placed apically to this coronal line in correlation with the implant's centre. The residual bone volume (BV) was determined by the ratio of the BV divided by the volume of interest. Each mouse represents a unit of analysis using the average BV of both implants. The analysis technique is further depicted in Appendix S1.

2.8 | Cytokine secretion by cultured splenocytes

Splenocytes were collected and seeded at 2×10^6 cells per well. The cells were cultured for 60 h either in the presence or absence of the *Pg* antigen, RgpA. The supernatants were collected and stored at −80°C, until further analysis.

2.9 | Cultivation of oral microbiota

Oral cavities of the mice were swabbed for 30 s. The samples were serially diluted and plated on TBS and blood agar under aerobic and anaerobic conditions, respectively, to determine the levels of total cultivatable oral bacteria.

2.10 | Taxonomic microbiota sequencing and analysis

Oral bacterial DNA was extracted using the MoBio Powersoil and Zymo Quick-DNA fungal\bacterial DNA extraction kits and used for Illumina sequencing. The alpha and beta diversities were calculated using the Shannon index and Bray–Curtis dissimilarity, respectively. For more details see Appendix S1.

2.11 | Statistical analysis

In each experiment, mice were individually tested, and data were expressed as mean ± SEM. For flow cytometry experiments, tissue from two animals were pooled and considered, $n = 1$. The calculation of the number of animals was based on previous study (Heyman et al., 2020), with a primary objective to detect mean difference in bone loss volume using micro-computed tomography (μCT). The analysis showed an ideal sample size of 10 mice per group to ensure 80% power with an α of .05. Statistical analyses were performed using one-way analysis of variance with Benferroni correction and Student's *t*-test via Prism 6.0 (GraphPad software); a $p < .05$ was considered significant. $^{*}p < .05$, $^{**}p < .01$, $^{***}p < .001$.

3 | RESULTS

3.1 | *Pg* infection drives periodontal bone loss around dental implants

Because the periodontal pathogen *Pg* is associated with human periodontitis (Hajishengallis et al., 2011) and peri-implantitis (Ata-Ali et al., 2015), we first examined whether infection with *Pg* will facilitate bone loss around implants, using the murine peri-implantitis model (Figure 1a). As depicted in Figure 1b, significant bone loss was detected around *Pg*-infected implants (peri-implantitis) as compared to sham-infected implants. We previously had shown that implants, themselves, promote bone loss around teeth that are located contra-laterally to the implants (Heyman et al., 2020); thus, we examined the effect of *Pg* infection on those teeth. Figure 1c shows that bacterial infection induced further bone loss around contra-lateral teeth of implanted mice (contra-lateral). We next evaluated the ratio between the expression of two key regulators of pathophysiological bone remodelling, namely the receptor activator of NF-κB ligand (RANKL), and its antagonist osteoprotegerin (OPG). Our results show that, following *Pg* infection, the RANKL/OPG ratio was

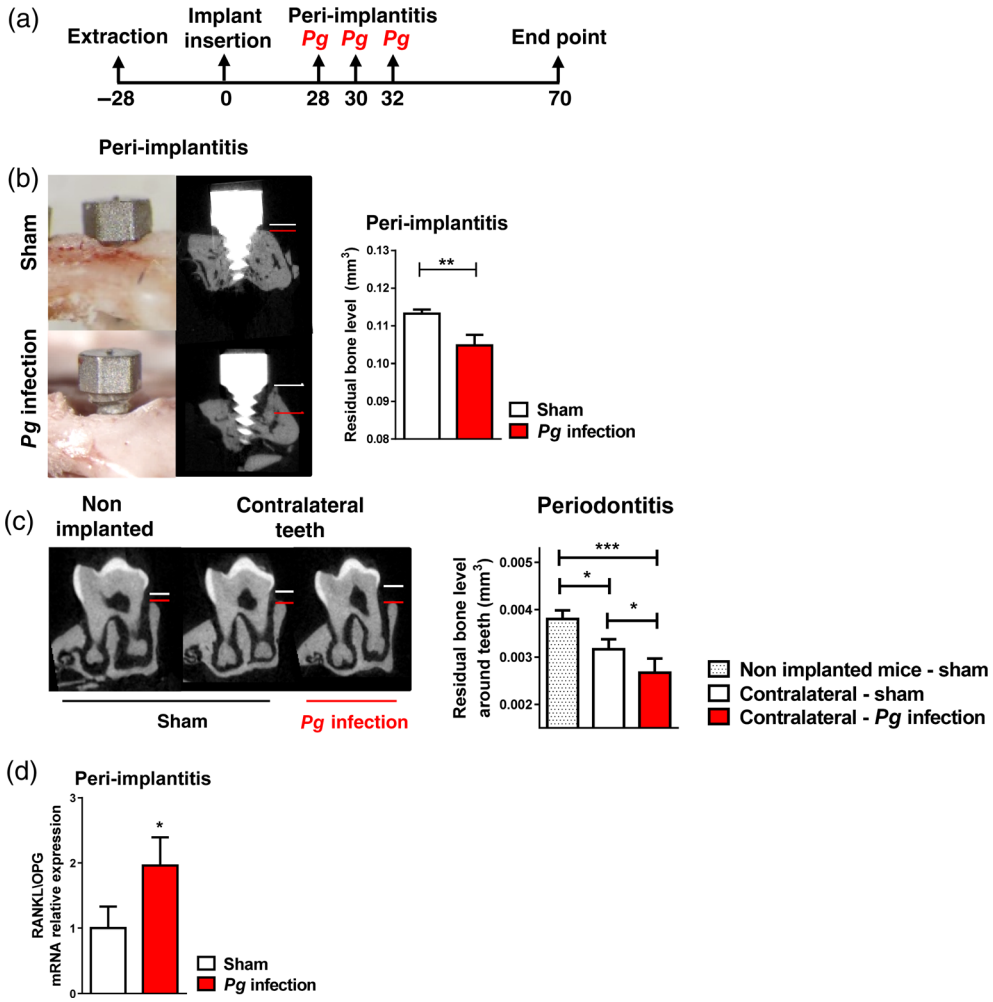

FIGURE 1 *Porphyromonas gingivalis* (*Pg*) infection promotes bone loss around dental implants and teeth. (a) Experimental design demonstrating the time points of oral infection post implant placement. (b) Representative clinical and micro-computed tomography (μCT) images taken 6 weeks after infection with *Pg* or administration of sham carboxymethyl cellulose. Bone loss is visible within the implant's neck area and is presented as the distance between the white line (cervical margin—baseline) and the red line (bone level). The accompanying bar graph demonstrates three-dimensional quantification analysis of the residual peri-implant bone volume after *Pg* infection or sham administration in 20 mice ($n = 10$ mice per group). Data are representative of one out of three independent experiments. (c) Representative μCT images of teeth from naïve mice and contra-lateral teeth to the implants taken 6 weeks after *Pg* infection or sham administration (periodontitis in contra-lateral teeth). Bone loss is visible between the white and red lines. Bar graph illustrates three-dimensional quantification analysis of the residual bone volume around teeth. Data are representative of one out of two independent experiment ($n = 6–9$ mice per group). (d) RANKL and OPG mRNA expression levels were quantified in the peri-implant mucosa of infected (peri-implantitis) and sham-infected implants using quantitative real-time polymerase chain reaction. Bar graphs present the fold change in RANKL/OPG expression ratio normalized to sham group and represent the mean values ± SEM ($n = 5$ per group, each sample represents oral tissues pooled from two individual mice). Data are representative of two experiments. *$p < .05$; **$p < .01$; ***$p < .001$. [Colour figure can be viewed at wileyonlinelibrary.com]

significantly elevated in the PIM (peri-implantitis) following *Pg* infection (Figure 1d). Taken together, our findings suggest that *Pg* is capable of driving peri-implantitis in murine dental implants, in accordance with its known association with human peri-implantitis.

3.2 | *Pg* infection dysregulates peri-implant immune response

We recently showed that dental implants dysregulate immune response in the PIM, leading to an influx of immune cells (Heyman et al., 2018). To examine whether *Pg* infection further impacts leukocyte infiltration, we analysed, using flow cytometry, gingival leukocytes that are known to play a role in periodontal bone remodelling (Mizraji et al., 2017). Based on the gating strategy described in Figure S1, increased levels of total leukocytes ($CD45^+$), neutrophils ($Ly6G^+Ly6C^+$), and monocytes ($CD11b^+Ly6C^{high\backslash low}$) were detected in the PIM, 6 weeks post infection, versus control, sham-infected tissue. In contrast, the percentage of antigen-presenting cells (APCs) ($MHCII^+CD11c^+$) was decreased (Figure 2a). Lymphocyte populations were also increased as a result of *Pg* infection, as reflected in significantly higher frequencies of T cells

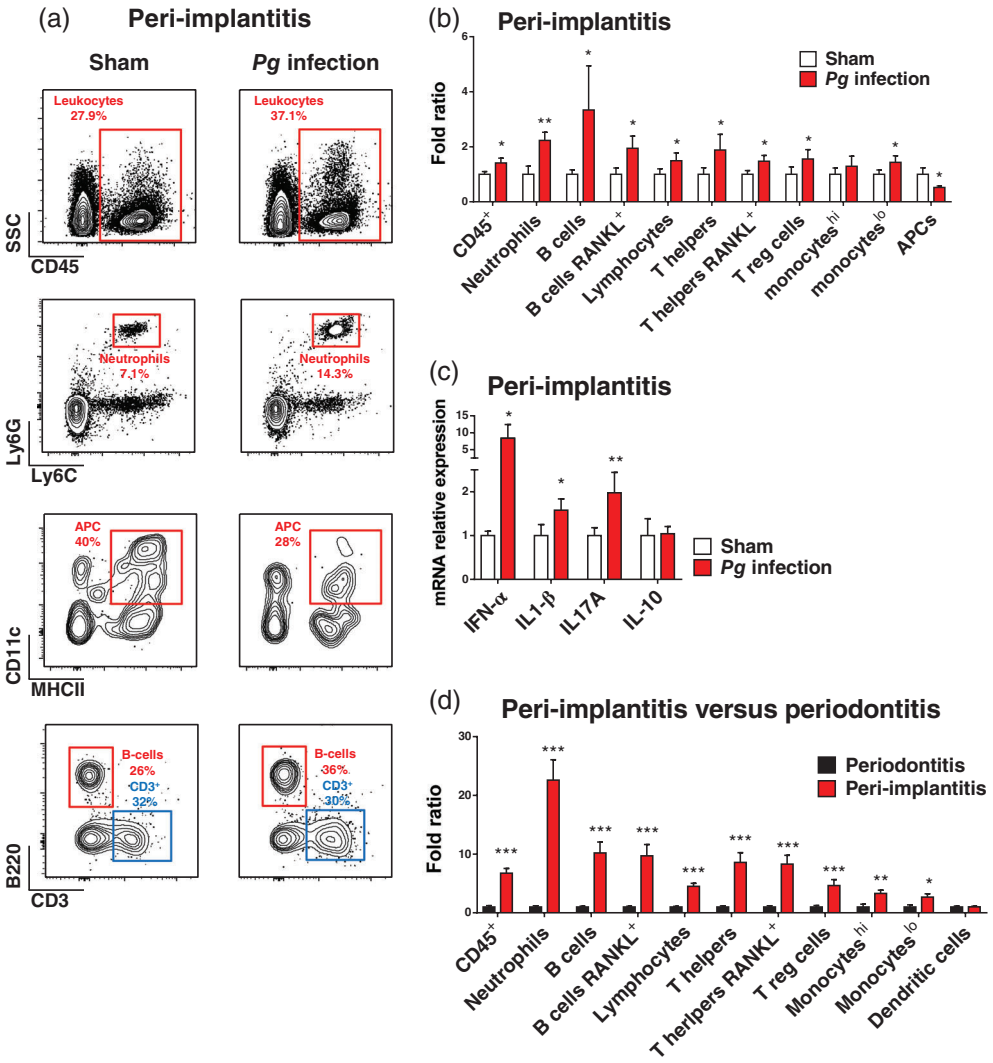

FIGURE 2 *Porphyromonas gingivalis* (*Pg*) infection exacerbates immune dysregulation around implants as compared to tissue surrounding teeth. (a) Representative fluorescence activated cell sorter (FACS) plots illustrate the percentage of each immune subset from within its parent gate. Following implant insertion and 6 weeks after infection with *Pg* or sham, the frequencies of $CD45^+$ leukocytes, B cells ($B220^+$), total lymphocytes ($CD3^+$), T helper cells ($CD3^+CD4^+$), Treg cells ($CD3^+CD4^+FOXP3^+$), RANKL-expressing T ($CD3^+CD4^+RANKL^+$) and B cells ($B220^+RANKL^+$), neutrophils ($Ly6G^+$ $Ly6C^+$), monocytes ($CD11b^+Ly6C^{high\backslash low}$), and antigen presenting cells (APCs) ($MHCII^+CD11c^+CD11b^+$) were calculated in the peri-implant mucosa. (b) Bar graph indicates fold change in the cell counts of each immune subtype in the peri-implant mucosa following infection or sham. The data are normalized to the sham-infected group ($n = 5$ per group, each sample represents oral tissues pooled from two individual mice). Data are representative of one out of two independent experiments. (c) mRNA expression levels of IFN-α, IL1-β, and IL-10 and IL17A in the peri-implantitis (PIM), 6 weeks following *Pg* infection or sham administration, as quantified by quantitative real-time polymerase chain reaction. Bar graph presents fold change in gene expression normalized to the sham-infected group and represents the mean values ± SEM ($n = 5$ per group, each sample represents oral tissues pooled from two individual mice). Data are representative of two experiments. (d) Immune cell subsets in the gingiva and PIM following *Pg* infection (experimental periodontitis vs. experimental peri-implantitis). Bar graphs indicates fold change in cell counts of each immune subtype, normalized to the experimental periodontitis group ($n = 5$ per group, each sample represents oral tissues pooled from two individual mice). Data are representative of one out of two independent experiments. $^*p < .05$; $^{**}p < .01$; $^{***}p < .001$. [Colour figure can be viewed at wileyonlinelibrary.com]

($CD3^+$), B cells ($B220^+$), T helper cells ($CD3^+CD4^+$), and T-regulatory cells ($CD3^+CD4^+FoxP3^+$) as compared to sham-infected mice (Figure 2b). Since RANKL expression on lymphocytes was reported to affect osteoclastogenesis and facilitate bone loss (Chen et al., 2014), we evaluated its expression on T and B cells following *Pg* infection. Concurring with our earlier results showing RANKL/OPG mRNA overexpression in peri-implantitis (Figure 1d), RANKL expression on $CD4^+$ T cells and B cells in the PIM was elevated post infection compared to sham-infected control (Figure 2b). To further examine the immunological status of the PIM, we quantified the expression of immune response-associated genes by RT-qPCR. As depicted in Figure 2c, the expressions of IFN-α, IL1-β, and IL-17 were up-regulated in the PIM of mice with peri-implantitis, while the difference in expression of IL-10 was insignificant. Since *Pg*

infection is known to elevate the inflammatory milieu in the gingiva around teeth (Hajishengallis et al., 2011) and our aforementioned results demonstrated a significant influx of immune cells to the PIM, we evaluated the difference in the level of immune cell invasion between experimental periodontitis and peri-implantitis. As shown in Figure 2d, an elevated influx of various leukocyte subsets was found in the peri-implantitis group compared to the periodontitis group. Of note, neutrophils and RANKL-expressing T and B cells were almost 25- and 10-fold higher, respectively, in peri-implantitis compared to periodontitis, suggesting a more aggressive and uncontrolled immune response in peri-implantitis. Taken together, these findings demonstrate that *Pg* infection results in a more aggravated inflammatory milieu around implants than around teeth, likely indicating the capacity of this pathogen to facilitate bone loss.

3.3 | *Pg* infection induces oral microbial dysbiosis in implanted and non-implanted mice

We next explored the effect of pathogen-associated dysregulation of oral immunity on the oral microbiome. For this, we sampled the oral microbiota at several time points, as depicted in Figure 3a. The levels of both cultivated anaerobic and aerobic bacteria were significantly higher around infected implants and teeth than in uninfected tissue

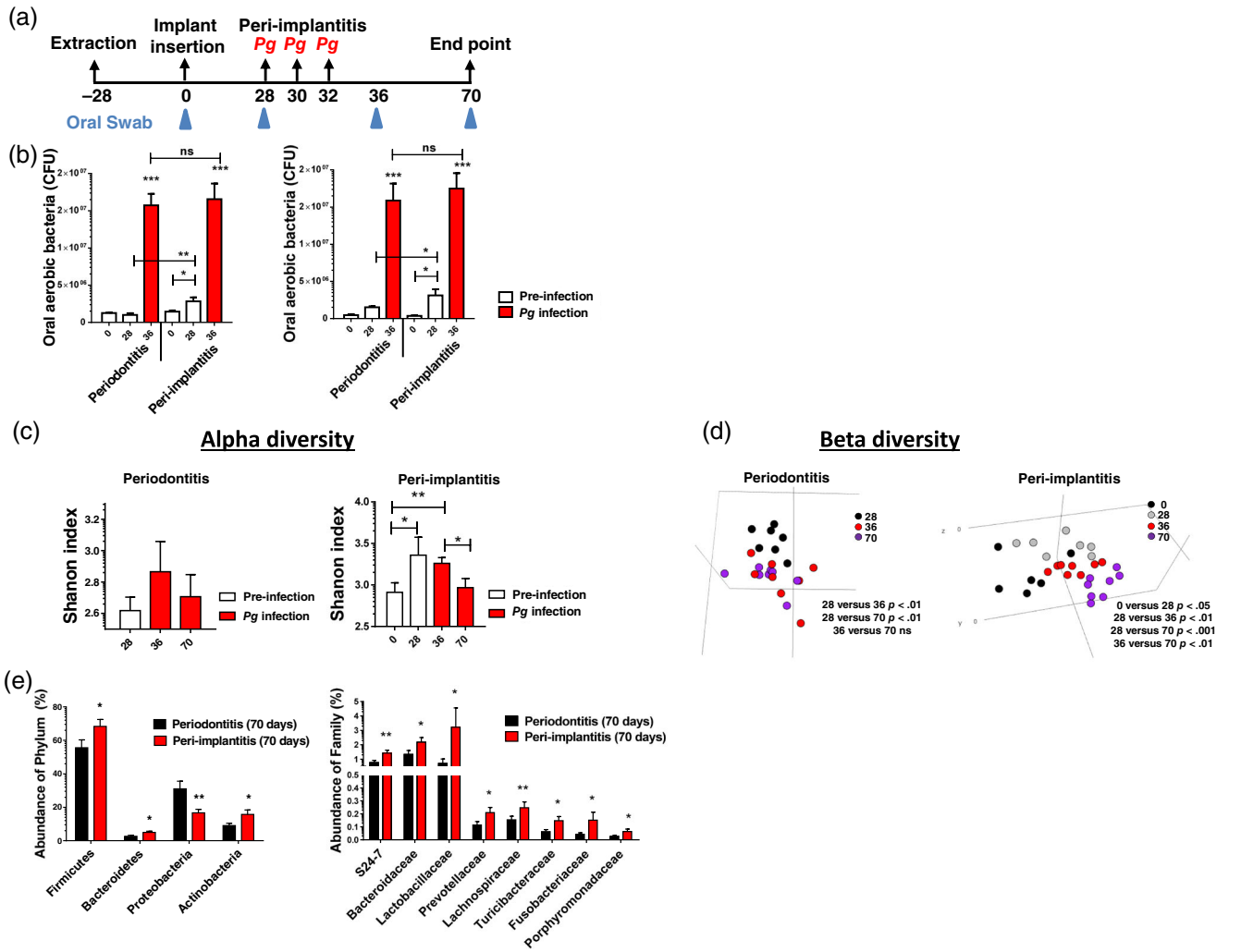

FIGURE 3 *Porphyromonas gingivalis* (*Pg*) infection induces dysbiosis of the oral microbiota in implanted and non-implanted mice. (a) Experimental design demonstrating the time points of oral swabs taken for bacterial analysis. (b) Colony forming unit of total cultivable oral aerobic and anaerobic bacteria at baseline (Day 0), following implant insertion, and before *Pg* infection (Day 28), and following infection (Day 36). Data are representative of two experiments ($n = 6$ mice per group). (c) Alpha diversity bar plot representing taxa richness before and after implant/teeth infection (peri-implantitis vs. periodontitis) using the Shannon index ($n = 6–8$ mice per time point). (d) 3D NMDS plots based on Bray–Curtis dissimilarity illustrates the bacterial community structure before and after implant insertion and *Pg* infection. PERMANOVA was used to assess significance between groups. Each dot represents the oral microbiome of one mouse. (e) Taxonomic analysis of the most abundant phyla and families in implanted and non-implanted mice (Day 70). Data represent two independent experiments. *p <.05; **p < .01; ***p < .001. [Colour figure can be viewed at wileyonlinelibrary.com]

(Day 36), without any differences between the groups (Figure 3b). Of note, the presence of implants in the oral cavity was sufficient to significantly increase the anaerobic and aerobic bacterial load (Day 28), as previously reported (Heyman et al., 2020). Further analysis revealed that the microbial diversity (alpha diversity) around teeth did not change significantly following infection and throughout the experiment. In contrast, the diversity around implants increased between Day 0 and Day 28 and later on decreased between Day 36 and Day 70, regardless of bacterial infection (Figure 3c). The composition of the microbiota around teeth changed only following infection (Day 36) and stayed steady up to Day 70, while around implants the variety changed following implant placement (Day 28), following the infection (Day 36), and at Day 70, suggesting a more unstable and dysbiotic microbiome in peri-implantitis than in periodontitis (Figure 3d). To further dissect the microbiome changes that occur following infection, we performed a detailed taxonomic analysis. Examining the

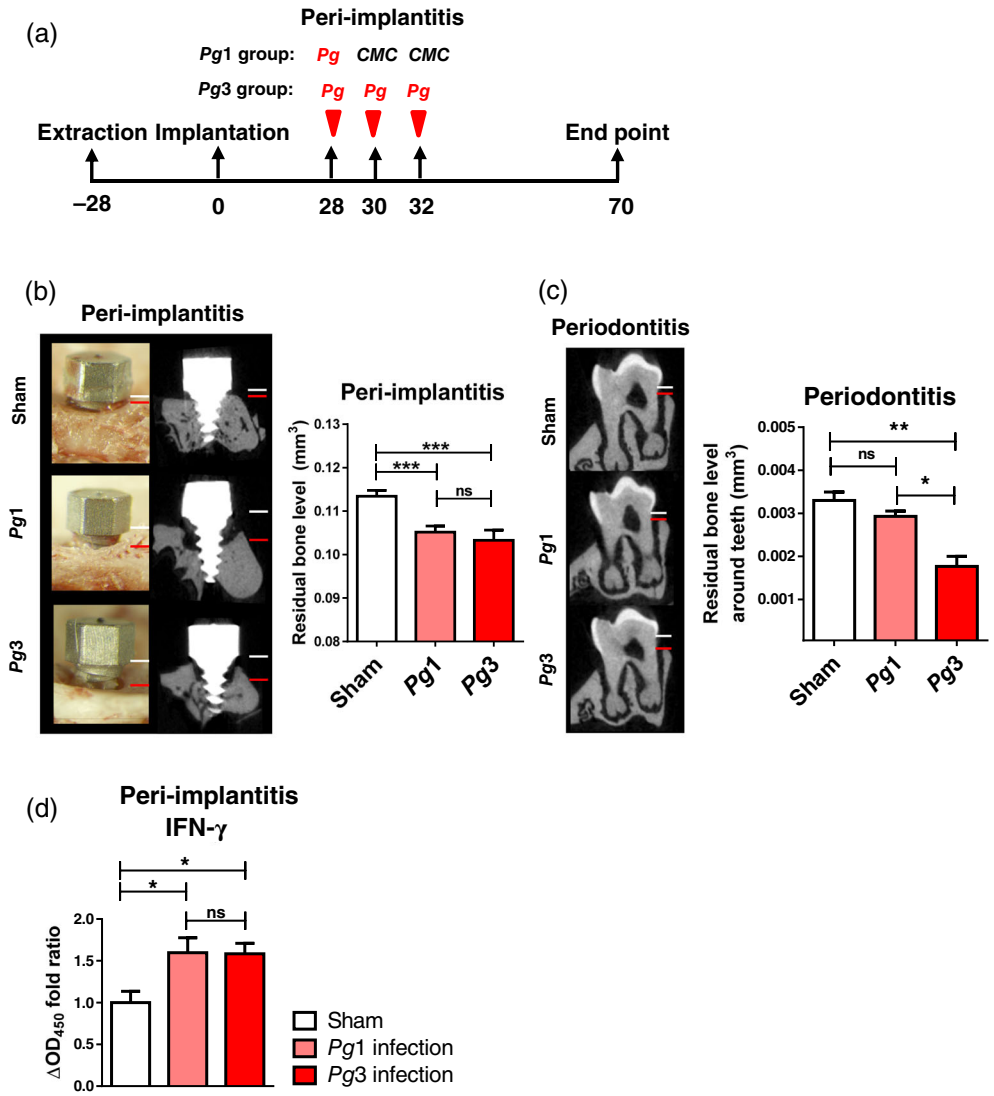

FIGURE 4 Implants are more susceptible to microbial dysbiosis than teeth. (a) Experimental design for repetitive (*Pg*3) versus single (*Pg*1) *Porphyromonas gingivalis* (*Pg*) infection model. (b) Representative clinical and micro-computed tomography (μCT) images taken post implant placement and 6 weeks after infection. Bone loss is presented as the distance between the white line (cervical margin—baseline) and the red line (bone level). Accompanying bar graph demonstrates three-dimensional quantification analysis of the residual peri-implant bone volume after *Pg* infection or CMC administration (sham) with a total of $n = 10$ mice per group. Data are representative of one out of two independent experiments. (c) Representative μCT images of the teeth in non-implanted group (periodontitis) taken 6 weeks after infection. Bone loss is represented as the distance between the white line and the red line. Bar graph illustrates three-dimensional quantification analysis of the residual bone volume around teeth with a total of $n = 6$–10 mice per group. Data are representative of one out of two independent experiments. (d) IFN-γ levels in the supernatants of splenocytes that were extracted from mice 6 weeks following implant infection. The cultured splenocytes were unstimulated or stimulated with RgpA, and IFN-γ levels were quantified by ELISA. Bar graph presents the mean values as the fold change in the delta optic density (OD) between stimulated and unstimulated splenocytes ± SEM ($n = 6$ mice per group). *$p < 0.5$; **$p < .01$; ***$p < .001$. [Colour figure can be viewed at wileyonlinelibrary.com]

abundance of different phyla and families 5 weeks following infection (Day 70), we found around implants increased abundance of most phyla and all families that were in a higher abundance in peri-implantitis patients than in periodontitis patients (Figure 3e). Overall, these findings suggest that *Pg* infection affects dysregulation of the implant-associated microbiota more than in periodontitis, resulting in a less stable and a more pathogen-enriched microbiota.

3.4 | Implants are more susceptible to *Pg*-induced bone loss than teeth

We previously demonstrated that repetitive infections rather than a single infection with *Pg* can induce bone loss around teeth in BALB/c mice (Mizraji et al., 2017). To examine whether the dysregulated immune responses developed around implants will impact their capability to respond to infection, we infected the mice with a single or repetitive *Pg* infections, as depicted in Figure 4a. μCT analysis revealed that a single infection (*Pg*1) was sufficient to induce significant bone loss around implants (Figure 4b), while repetitive infections (*Pg*3) were required to promote bone loss around teeth in non-implanted mice (Figure 4c), suggesting that implants are more susceptible to microbial challenge. Of note, single (*Pg*1) and repetitive infections (*Pg*3) both resulted in similar bone loss around implants (Figure 4b). Furthermore, repetitive infections resulted in significant bone loss around teeth regardless of the presence of an implant (data not shown). To examine systemic T-cell immunity, we harvested splenocytes from each group, re-stimulated them ex vivo with the *Pg* antigen RgpA, and measured IFN-γ levels using ELISA. Figure 4d shows that splenocytes isolated from single or repetitively infected and implanted mice secreted higher IFN-γ levels than from splenocytes isolated from sham-infected mice (Figure 4d).

3.5 | RvD2 prevents experimental peri-implantitis

Treatment with RvD2 was shown to reduce local neutrophil numbers and inhibit systemic and gingival Th1-type adaptive immune responses that mediate alveolar bone loss around teeth. RvD2 was also shown to protect against experimental periodontitis (Mizraji et al., 2018). Therefore, we sought to assess its efficacy as a treatment modality for peri-implantitis. Towards this end, we repetitively administered RvD2 to our peri-implantitis model at the times points and in doses depicted in Figure 5a. Initially, we evaluated bone loss around the implants and found that RvD2 treatment completely prevented bone loss (Figure 5b). Next, we examined the neutrophils in the tissue, and observed that RvD2 inhibited their invasion to the peri-implant tissue following infection (Figure 5c). Moreover, flow cytometry analysis showed that RvD2 treatment attenuated the influx of leukocytes, B cells, T cells, T helper cells, and RANKL-expressing T cells (Figure 5d). No change in monocytes and RANKL-expressing B cells was observed (data not shown). Lastly, we examined the systemic effect of RvD2 treatment by measuring the levels of IFN-γ secreted by isolated splenocytes. RvD2 treatment prevented the increase in levels of IFN-γ secreted by splenocytes from the peri-implantitis group (Figure 5e), emphasizing the inhibitory systemic effect of RvD2 on T-cell priming. To further validate the systemic effects, we analysed the cervical LNs for the presence of plasmacytoid dendritic cells (pDCs), because the accumulation of these cells in the LNs promotes alveolar bone loss through Th1-type immunity (Mizraji et al., 2017). Using flow cytometry and the gating strategy depicted in Figure S1, we found that RvD2 treatment prevented the increased frequency of pDCs ($MHCII^{low}CD11c^{int}CD11b^{-}B220^{+}PDCA1^{+}Siglec^{-}$) detected in the untreated peri-implantitis group (Figure 5f). Because migratory dendritic cells (mDCs) in the LNs are the sole subset capable of presenting antigen to T helper cells, we were interested in measuring the frequency of these cells in LNs. Our results show that, although mDCs increased significantly following infection, RvD2 treatment prevented their influx into the LNs. Importantly, the reduced frequencies of APCs around implants (Figure 2a) could be explained by the increased migration of DCs ($MHCII^{high}CD11c^{+}$) into the LNs. Collectively, these results suggest that RvD2 prevents alveolar bone loss by modulating local and systemic immunity.

4 | DISCUSSION

The present study describes the immune mechanisms and microbiome around dental implants in a model of murine peri-implantitis. We had previously shown that dental implants not only dysregulate local immunity but also elicit a broader effect on remote sites via microbial dysbiosis and alteration of the systemic immune response (Heyman et al., 2018, 2020). Here we demonstrated that oral microbial dysbiosis induced by *Pg* infection facilitates bone loss around implants and teeth by dysregulating the more delicate immune homeostasis that exists following implant placement. The observed bone loss was accompanied by a higher RANKL/OPG ratio in the tissue around the diseased implants and by an influx of immune cells into the PIM. When compared to periodontitis, the PIM surrounding diseased implants demonstrated higher accumulation of immune cells, in particular, neutrophils, T helper cells, B cells, monocytes, and RANKL-expressing T and B cells. These findings are in agreement with those of human studies showing that the ICT in peri-implantitis has a significantly larger number of total inflammatory cells and more immune cells, such as T cells, plasma cells, B cells (Bullon et al., 2004), and neutrophils (Berglundh et al., 2011; Carcuac & Berglundh, 2014) compared to the ICT in periodontitis. The present observations support our earlier findings and underline the relevance of our model to the clinical setting. Furthermore, the expression of key cytokines related to periodontal disease and tissue damage, such as IFN-α and IL-1β, was higher in the peri-implantitis group than in the control group. The role of type I interferons (IFN-I) on immunological dysfunction in our peri-implantitis model is probably central, as it increases almost 10-fold around infected implants compared to around sham-infected implants. Mizraji et al. (2017) recently demonstrated the connection between the accumulation of pDCs (the major IFN-α producers in the LNs), elevated IFN

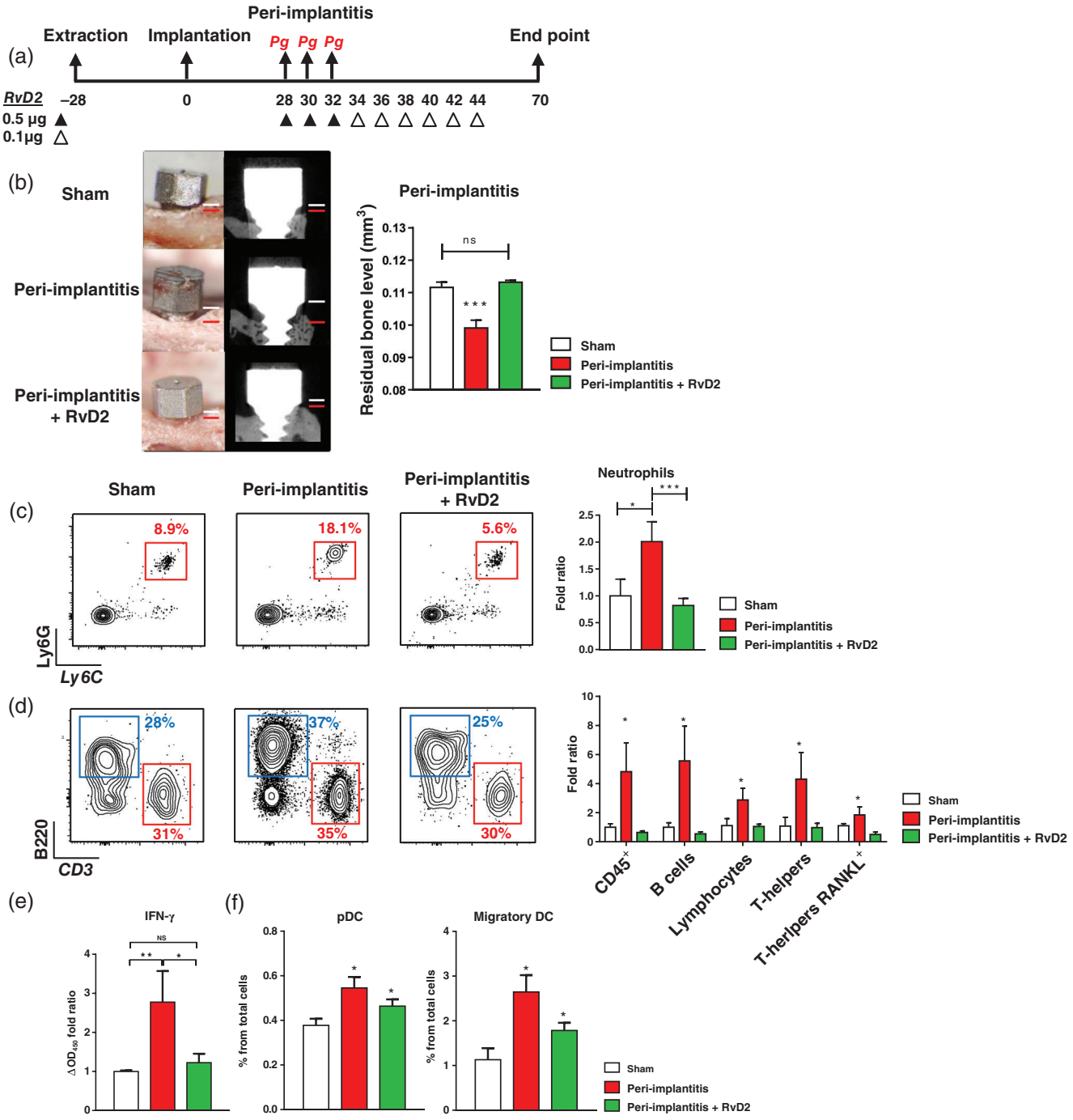

FIGURE 5 Treatment with Resolvin-D2 (RvD2) prevents experimental peri-implantitis. (a) Experimental design of treatment with RvD2. (b) Representative clinical, micro-computed tomography images and 3D quantification analysis of the residual peri-implant bone, $n = 5–6$ mice per group. Data are representative of one out of two experiments. (c,d) Representative fluorescence activated cell sorter (FACS) plots illustrate the incidence of (c) neutrophils ($Ly6G^+Ly6C^+$) and (d) B and T cells ($B220^+$, $CD3^+$) 6 weeks after infection, with or without RvD2 treatment. Bar graphs present fold change in the frequencies of different immune subsets from total counts, normalized to the sham group, presented as mean values ± SEM ($n = 4$ per group, each sample represents tissues pooled from two individual mice). Data are representative of one out of two experiments. (e) IFN-γ levels in the supernatants of unstimulated cultured splenocytes extracted from infected mice, with or without RvD2 treatment, were quantified by ELISA. Bar graph presents mean values ± SEM ($n = 6$ mice per group). (f) Frequency of plasmacytoid dendritic cells (pDCs) and migratory dendritic cells (DCs) extracted from the lymph nodes of mice, 6 weeks after infection. Mice received RvD2 treatment according to the experimental design as detailed in (a). Bar graphs demonstrate the fold change of different immune cells from total cell counts, normalized to the sham group and presented as mean values ± SEM ($n = 4$ mice per group). Data are representative of one out of two experiments. *$p < .05$; **$p < .01$; ***$p < .001$. [Colour figure can be viewed at wileyonlinelibrary.com]

expression in tissue, and increased proportions of $CD4^+$ $RANKL^+$ cells to bone loss in a model of murine periodontitis (). This might also be a possible immune mechanism in our peri-implantitis model, as we measured increased proportions of pDC in the LNs, more $CD4^+$ $RANKL^+$ cells in the PIM, and increased expression of IFN-α around infected implants. The reduction of APCs in the PIM post infection and an increased proportion of migratory DCs in the cervical LNs suggest increased activation and/or migration of DCs from the diseased implant sites to the LNs, perhaps due to a high antigen load or a change in the microbiome composition. In concurrence with this assumption, the high levels of activated splenocytes in the peri-implantitis group might also be due to increased exposure to IFN-I, which activates APCs (Montoya et al., 2002) to present antigens from the dysbiotic microbiota for long periods.

Pg is an anaerobic, gram-negative bacterium associated with peri-implantitis and periodontitis. This bacterium is often referred to as a "key-stone pathogen" (Hajishengallis et al., 2012), as it can enhance the survival of other oral bacteria and cause dysbiosis, which results in immune dysregulation and enhanced tissue and bone deterioration (Hajishengallis et al., 2011). We recently published the use of *Pg* for induction of experimental peri-implantitis in a mouse model (Tzach-Nahman et al., 2017). Similar to these earlier findings, *Pg* infection resulted in increased anaerobic bacterial counts. Our data indicating that the bacterial diversity around implants increased significantly following implant placement but not following *Pg* infection are in accordance with previous human studies presenting similar diversity in healthy and diseased implants (Yu et al., 2019). In terms of variety, we found that although around implants the variety was different at all time points, around teeth only *Pg* infection changed the variety, which stayed the same afterwards, suggesting a steady homeostasis around teeth but not around implants. Our detailed taxonomic analysis revealed higher relative abundance of known periodontal pathogenic and inflammophilic phyla and families in the peri-implantitis group than in the periodontitis group, as previously reported in humans (Kumar et al., 2012; Winter & Bäumler, 2014; Colombo & Tanner, 2019).

Recently, we demonstrated that Langerhans cell differentiation is impaired in the PIM epithelium, leading to dysregulated immunity that shifts towards chronic inflammation and tissue destruction (Heyman et al., 2018). Therefore, we hypothesized that this dysregulated immune homeostasis in tissue around implants is more susceptible to infection and deterioration than healthy teeth. To address this question, we infected the mice with a single dose of *Pg*, known not to mediate bone loss around teeth (Mizraji et al., 2017), or with repetitive *Pg* infections. Our results show that a single infection was sufficient to promote bone loss around implants but not around healthy teeth, emphasizing the more fragile immune homeostasis around implants. Moreover, the increased expression of IL-17A and especially IFN-α in non-infected implants (Heyman et al., 2020) also strengthens our hypothesis that the inflammatory milieu around steady-state implants is dysregulated and more activated than around healthy teeth. Importantly, repetitive infections resulted in significant bone loss around teeth, regardless of implant presence, suggesting that the clinical effects caused by repetitive *Pg* infections to teeth are greater than the effects caused by implants (data not shown). This result further strengthens our hypothesis that bone loss around contra-lateral teeth results from microbial dysbiosis. Collectively, these findings are in agreement with the aggressive nature of peri-implantitis compared to periodontitis observed in human patients (Salvi et al., 2017).

Although neutrophils play an essential role in host defence, chronic accumulation and prolonged activation of neutrophils can lead to tissue injury during periodontitis. We had shown previously that, while total leukocytes and B and $CD4^+$ T lymphocytes (independent of RANKL expression) were considerably reduced around implants following broad spectrum antibiotic treatment, neutrophils were not altered by antibiotics, suggesting that they may play an important role in the pathogenesis of peri-implantitis (Heyman et al., 2020). In the current work, we found that neutrophils were present in 25-fold more frequent around infected implants (peri-implantitis) than in the vicinity of infected teeth (periodontitis) and that IFN-α was expressed at a 10-fold higher level around infected implants. Since our previous work had shown that RvD2 treatment prevented endothelial transmigration of neutrophils from the circulation into the gingiva and inhibited systemic and gingival Th1-type adaptive responses that are known to mediate alveolar bone loss around teeth (Mizraji et al., 2018), we tested its efficacy in preventing peri-implantitis. Our data here show that treatment with RvD2 prevented bone loss around infected implants. This finding could be explained by its ability to reduce the accumulation of neutrophils and B cells, both of which are known to have an important role in the pathogenesis of periodontitis (Hajishengallis & Korostoff, 2015; Hajishengallis et al., 2016). Furthermore, RvD2 treatment reduced the frequency of gingival lymphocytes, RANKL-expressing $CD4^+$ cells, pDCs, and migratory DC in the LNs and decreased the basal secretion of IFN-γ from splenocytes. Taken together, these data suggest that, in the experimental peri-implantitis model, RvD2 restrains innate and adaptive responses that are also known to mediate alveolar bone loss in this murine model.

In summary, this study shows that the dysregulated homeostasis around implants is fragile and more susceptible to alveolar bone loss following microbial dysbiosis. We also showed the efficacy of treatment with RvD2, which prevented peri-implantitis, most likely by attenuating the influx of neutrophils and other immune cell populations to the gingiva and pDCs to the LNs.

AUTHOR CONTRIBUTIONS

Oded Heyman designed and performed the study, analyzed the data, and drafted the manuscript. Yael Horev performed the study, analyzed the data, and drafted the manuscript. Gabriel Mizraji analyzed the data and drafted the manuscript. Yaron Haviv analyzed the data, and drafted and critically revised the manuscript. Lior Shapira designed the study, analyzed the data, and drafted and critically revised the manuscript. Asaf Wilensky designed the study, analyzed the data, and wrote the manuscript.

ACKNOWLEDGEMENTS

This work was supported in part by the Israel Science Foundation Grant 2369/18, awarded to Asaf Wilensky. We would like to thank MIS Implants Technologies for manufacturing the micro-implants.

CONFLICT OF INTEREST

The authors declare no conflict of interests.

DATA AVAILABILITY STATEMENT

The data that support the findings of this study are available from the corresponding author upon reasonable request.

ETHICS STATEMENT

All experimental procedures were reviewed and approved by the IACUC of the Hadassah-Hebrew University Medical Center.

ORCID

Lior Shapira https://orcid.org/0000-0001-9145-5155
Asaf Wilensky https://orcid.org/0000-0001-9002-6041

REFERENCES

Ata-Ali, J., Flichy-Fernández, A. J., Alegre-Domingo, T., Ata-Ali, F., Palacio, J., & Peñarrocha-Diago, M. (2015). Clinical, microbiological, and immunological aspects of healthy versus peri-implantitis tissue in full arch reconstruction patients: A prospective cross-sectional study. *BMC Oral Health*, *15*, 43. https://doi.org/10.1186/s12903-015-0031-9

Berglundh, T., Armitage, G., Araujo, M. G., Avila-Ortiz, G., Blanco, J., Camargo, P. M., Chen, S., Cochran, D., Derks, J., Figuero, E., Hämmerle, C. H. F., Heitz-Mayfield, L. J. A., Huynh-Ba, G., Iacono, V., Koo, K.-T., Lambert, F., McCauley, L., Quirynen, M., Renvert, S., … Zitzmann, N. (2018). Peri-implant diseases and conditions: Consensus report of workgroup 4 of the 2017 World Workshop on the Classification of Periodontal and Peri-Implant Diseases and Conditions. *Journal of Clinical Periodontology*, *45*, S286–S291. https://doi.org/10.1111/jcpe.12957

Berglundh, T., Zitzmann, N. U., & Donati, M. (2011). Are peri-implantitis lesions different from periodontitis lesions? *Journal of Clinical Periodontology*, *38*, 188–202. https://doi.org/10.1111/j.1600-051X.2010.01672.x

Bullon, P., Fioroni, M., Goteri, G., Rubini, C., & Battino, M. (2004). Immunohistochemical analysis of soft tissues in implants with healthy and peri-implantitis condition, and aggressive periodontitis. *Clinical Oral Implants Research*, *15*, 553–559. https://doi.org/10.1111/j.1600-0501.2004.01072.x

Carcuac, O., & Berglundh, T. (2014). Composition of human peri-implantitis and periodontitis lesions. *Journal of Dental Research*, *93*, 1083–1088. https://doi.org/10.1177/0022034514551754

Chen, B., Wu, W., Sun, W., Zhang, Q., Yan, F., & Xiao, Y. (2014). RANKL expression in periodontal disease: Where does RANKL come from? *BioMed Research International*, *2014*, 731039. https://doi.org/10.1155/2014/731039

Chiurchiù, V., Leuti, A., Dalli, J., Jacobsson, A., Battistini, L., Maccarrone, M., & Serhan, C. N. (2016). Proresolving lipid mediators resolvin D1, resolvin D2, and maresin 1 are critical in modulating T cell responses. *Science Translational Medicine*, *8*, 353ra111. https://doi.org/10.1126/scitranslmed.aaf7483

Colombo, A. P. V., & Tanner, A. C. R. (2019). The role of bacterial biofilms in dental caries and periodontal and peri-implant diseases: A historical perspective. *Journal of Dental Research*, *98*, 373–385. https://doi.org/10.1177/0022034519830686

Derks, J., & Tomasi, C. (2015). Peri-implant health and disease. A systematic review of current epidemiology. *Journal of Clinical Periodontology*, *42*(Suppl. 16), S158–S171. https://doi.org/10.1111/jcpe.12334

Hajishengallis, G., Darveau, R. P., & Curtis, M. A. (2012). The keystone-pathogen hypothesis. *Nature Reviews Microbiology*, *10*, 717–725. https://doi.org/10.1038/nrmicro2873

Hajishengallis, G., & Korostoff, J. M. (2015). Response to comment on "the B cell-stimulatory cytokines BLyS and APRIL are elevated in human periodontitis and are required for B cell-dependent bone loss in experimental murine periodontitis". *Journal of Immunology*, *195*, 5099–5100. https://doi.org/10.4049/jimmunol.1502066

Hajishengallis, G., Liang, S., Payne, M. A., Hashim, A., Jotwani, R., Eskan, M. A., McIntosh, M. L., Alsam, A., Kirkwood, K. L., Lambris, J. D., Darveau, R. P., & Curtis, M. A. (2011). Low-abundance biofilm species orchestrates inflammatory periodontal disease through the commensal microbiota and complement. *Cell Host & Microbe*, *10*, 497–506. https://doi.org/10.1016/j.chom.2011.10.006

Hajishengallis, G., Moutsopoulos, N. M., Hajishengallis, E., & Chavakis, T. (2016). Immune and regulatory functions of neutrophils in inflammatory bone loss. *Seminars in Immunology*, *28*, 146–158. https://doi.org/10.1016/j.smim.2016.02.002

Hasturk, H., Kantarci, A., Goguet-Surmenian, E., Blackwood, A., Andry, C., Serhan, C. N., & Van Dyke, T. E. (2007). Resolvin E1 regulates inflammation at the cellular and tissue level and restores tissue homeostasis in vivo. *Journal of Immunology*, *179*, 7021–7029. https://doi.org/10.4049/jimmunol.179.10.7021

Heyman, O., Horev, Y., Koren, N., Barel, O., Aizenbud, I., Aizenbud, Y., Brandwein, M., Shapira, L., Hovav, A. H., & Wilensky, A. (2020). Niche specific microbiota-dependent and independent bone loss around dental implants and teeth. *Journal of Dental Research*, *99*, 1092–1101. https://doi.org/10.1177/0022034520920577

Heyman, O., Koren, N., Mizraji, G., Capucha, T., Wald, S., Nassar, M., Tabib, Y., Shapira, L., Hovav, A. H., & Wilensky, A. (2018). Impaired differentiation of Langerhans cells in the murine oral epithelium adjacent to titanium dental implants. *Frontiers in Immunology*, *9*, 1712. https://doi.org/10.3389/fimmu.2018.01712

Kotsakis, G. A., & Olmedo, D. G. (2021). Peri-implantitis is not periodontitis: Scientific discoveries shed light on microbiome-biomaterial interactions that may determine disease phenotype. *Periodontology 2000*, *86*, 231–240. https://doi.org/10.1111/prd.12372

Koutouzis, T., Eastman, C., Chukkapalli, S., Larjava, H., & Kesavalu, L. (2017). A novel rat model of polymicrobial peri-implantitis: A preliminary study. *Journal of Periodontology*, *88*, e32–e41. https://doi.org/10.1902/jop.2016.160273

Kumar, P. S., Mason, M. R., Brooker, M. R., & O'Brien, K. (2012). Pyrosequencing reveals unique microbial signatures associated with healthy and failing dental implants. *Journal of Clinical Periodontology*, *39*, 425–433. https://doi.org/10.1111/j.1600-051X.2012.01856.x

Mizraji, G., Heyman, O., Van Dyke, T. E., & Wilensky, A. (2018). Resolvin D2 restrains Th1 immunity and prevents alveolar bone loss in murine periodontitis. *Frontiers in Immunology*, *9*, 785. https://doi.org/10.3389/fimmu.2018.00785

Mizraji, G., Nassar, M., Segev, H., Sharawi, H., Eli-Berchoer, L., Capucha, T., Nir, T., Tabib, Y., Maimon, A., Dishon, S., Shapira, L., Nussbaum, G., Wilensky, A., & Hovav, A. H. (2017). *Porphyromonas gingivalis* promotes unrestrained type I interferon production by dysregulating TAM signaling via MYD88 degradation. *Cell Reports*, *18*, 419–431. https://doi.org/10.1016/j.celrep.2016.12.047

Montoya, M., Schiavoni, G., Mattei, F., Gresser, I., Belardelli, F., Borrow, P., & Tough, D. F. (2002). Type I interferons produced by dendritic cells promote their phenotypic and functional activation. *Blood*, *99*, 3263–3271. https://doi.org/10.1182/blood.V99.9.3263

Pirih, F. Q., Hiyari, S., Leung, H. Y., Barroso, A. D., Jorge, A. C., Perussolo, J., Atti, E., Lin, Y. L., Tetradis, S., & Camargo, P. M. (2015). A murine model of lipopolysaccharide-induced peri-implant mucositis and peri-implantitis. *The Journal of Oral Implantology*, *41*, e158–e164. https://doi.org/10.1563/aaid-joi-D-14-00068

Renvert, S., Roos-Jansaker, A. M., & Claffey, N. (2008). Non-surgical treatment of peri-implant mucositis and peri-implantitis: A literature

review. *Journal of Clinical Periodontology*, *35*, 305–315. https://doi.org/10.1111/j.1600-051X.2008.01276.x

Salvi, G. E., Cosgarea, R., & Sculean, A. (2017). Prevalence and mechanisms of peri-implant diseases. *Journal of Dental Research*, *96*, 31–37. https://doi.org/10.1177/0022034516667484

Serhan, C. N., Chiang, N., & Van Dyke, T. E. (2008). Resolving inflammation: Dual anti-inflammatory and pro-resolution lipid mediators. *Nature Reviews. Immunology*, *8*, 349–361. https://doi.org/10.1038/nri2294

Tzach-Nahman, R., Mizraji, G., Shapira, L., Nussbaum, G., & Wilensky, A. (2017). Oral infection with *Porphyromonas gingivalis* induces peri-implantitis in a murine model: Evaluation of bone loss and the local inflammatory response. *Journal of Clinical Periodontology*, *44*, 739–748. https://doi.org/10.1111/jcpe.12735

Van Dyke, T. E. (2020). Shifting the paradigm from inhibitors of inflammation to resolvers of inflammation in periodontitis. *Journal of Periodontology*, *91*(Suppl. 1), S19–s25. https://doi.org/10.1002/jper.20-0088

Wilensky, A., Tzach-Nahman, R., Potempa, J., Shapira, L., & Nussbaum, G. (2015). *Porphyromonas gingivalis* gingipains selectively reduce CD14 expression, leading to macrophage hyporesponsiveness to bacterial infection. *Journal of Innate Immunity*, *7*, 127–135. https://doi.org/10.1159/000365970

Winter, S. E., & Bäumler, A. J. (2014). Dysbiosis in the inflamed intestine: Chance favors the prepared microbe. *Gut Microbes*, *5*, 71–73. https://doi.org/10.4161/gmic.27129

Yu, X.-L., Chan, Y., Zhuang, L., Lai, H.-C., Lang, N. P., Keung Leung, W., & Watt, R. M. (2019). Intra-oral single-site comparisons of periodontal and peri-implant microbiota in health and disease. *Clinical Oral Implants Research*, *30*, 760–776. https://doi.org/10.1111/clr.13459

SUPPORTING INFORMATION

Additional supporting information may be found in the online version of the article at the publisher's website.

How to cite this article: Heyman, O., Horev, Y., Mizraji, G., Haviv, Y., Shapira, L., & Wilensky, A. (2022). Excessive inflammatory response to infection in experimental peri-implantitis: Resolution by Resolvin D2. *Journal of Clinical Periodontology*, 1–12. https://doi.org/10.1111/jcpe.13631